

Disturbance rejection control in real-time hybrid simulation of vehicle-bridge coupling vibration

*Ping Shao¹⁾, Wei Guo²⁾ and Qi Lei³⁾

^{1), 2)} *School of Civil Engineering, Central South University, Changsha, China*

³⁾ *School of Automation, Central South University, Changsha, China*

²⁾ guowei@csu.edu.cn

ABSTRACT

Real-time hybrid simulation (RTHS) technology can be adopted instead of ordinary large-scale field test for studying the vehicle-bridge coupling vibration of high-speed railway. In RTHS, the coupling structure is decomposed into experimental and numerical substructures that interact with each other through a loading device. Signal tracking accuracy of the loading device is distinctly affected by the experimental substructure, which further influences RTHS results. Therefore, a disturbance rejection control algorithm composed is proposed to solve this problem by compensating the equivalent disturbance of the experimental substructure. Effectiveness of the proposed control is verified on the RTHS model of high-speed railway vehicle-bridge coupling vibration.

1. INTRODUCTION

When a train passes bridge at high speed, vehicle-bridge coupling vibration affects moving stability and safety of the train, which is a critical part of related research. It is necessary to investigate this problem through physical experiments for reproducing the dynamic performance of the train and bridge (Xia 2018).

Real-time hybrid simulation (RTHS) is an efficient and cost-effective method to study dynamic characteristics of large-scale structures (Qian 2014). Taken train as experimental substructure and bridge as numerical substructure, the vehicle-bridge coupling vibration can be studied by the RTHS, where the shaking table is applied as the loading device of the experimental substructure. The shaking table excites the vehicle by following the track displacement output from the numerical analysis of the bridge. The coupling between experimental substructure and shaking table, which is known as control-structure interaction (Dyke 1995), challenges high-accuracy signal tracking of shaking table. Currently, there are two strategies to solve this problem: (1) designing control for the whole plant of shaking table and experimental substructure; (2) taking

¹⁾ Graduate Student

²⁾ Professor

³⁾ Associate Professor

shaking table as the controlled plant and compensating the disturbance brought by experimental substructure.

Varies applications of the first strategy improve the tracking accuracy of shaking table (Yang 2015, Ryu 2017). However, due to the difficulty of accurate modeling of experimental substructure and the complexity of tuning control for every test structure, it was mainly adopted in experimental research. In the second strategy, the controller is designed utilizing data measured by sensors on shaking table, and modeling experimental substructure is avoided. The most widely used control algorithm of strategy (2) is the disturbance observer-based practical control proposed by Iwasaki (2005), which is carried out for dual shaking tables by Li (2018). In this algorithm, the disturbance is compensated by inverse the interaction function between test structure and shaking table, which may be unstable because the degree of numerator exceeds the degree of denominator in the inverse model.

In this paper, a disturbance rejection control is proposed to improve the tracking accuracy of shaking table by computing the equivalent input disturbance of experimental substructure. Details of the proposed control are given in the second section. In the third section, a real-time hybrid simulation model of high-speed vehicle-bridge coupling vibration is conducted to verify the efficiency of the proposed control strategy. Finally, the verification results are discussed and summarized.

2. DISTURBANCE REJECTION CONTROL

The effect of experimental substructure on shaking table is regarded as a disturbance. An improved shaking table is constructed by inserting a disturbance compensator, which rejects the equivalent disturbance in the original shaking table. An outer-loop controller is designed to maintain the tracking accuracy of the improved shaking table. The disturbance compensator and the outer-loop controller formed the disturbance rejection control, of which the framework is shown in Fig. 1.

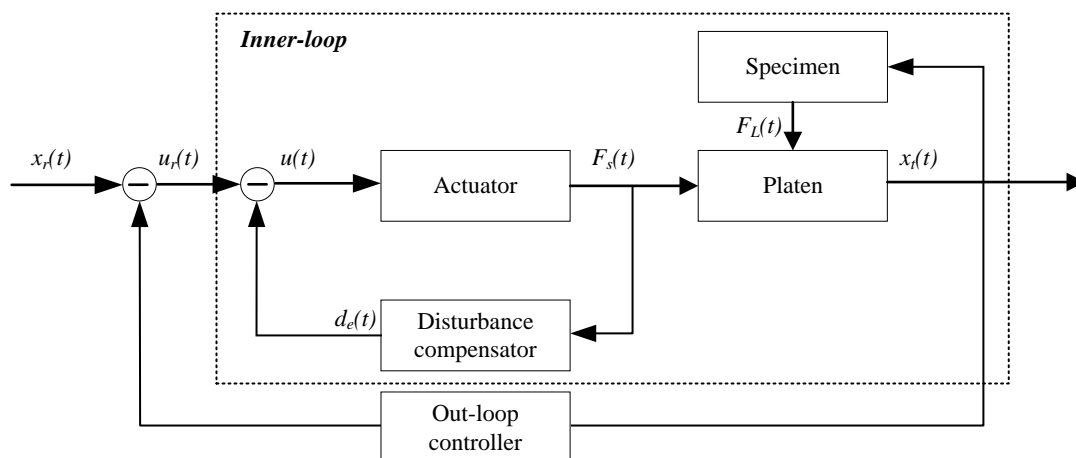


Fig. 1 Framework of disturbance rejection control

2.1 Equivalent disturbance

Consider the linear single-input single-output (SISO) plant

$$\begin{cases} \dot{x}_o(t) = \mathbf{A}x_o(t) + \mathbf{B}u(t) + \mathbf{B}_d d(t) \\ y_o(t) = \mathbf{C}x_o(t) \end{cases}, \quad (1)$$

where $\mathbf{A} \in \mathbb{R}^{n \times n}$, $\mathbf{B} \in \mathbb{R}^{n \times 1}$, $\mathbf{B}_d \in \mathbb{R}^{n \times 1}$, $\mathbf{C} \in \mathbb{R}^{1 \times n}$, $x_o(t) \in \mathbb{R}^n$, $u(t) \in R$, $d(t) \in R$, and $y_o(t) \in R$. The plant is controllable and observable, and it has no zeros on the imaginary axis. If the disturbance is assumed that it imposed only on the control input channel, then the plant is given by

$$\begin{cases} \dot{x}(t) = \mathbf{A}x(t) + \mathbf{B}[u(t) + d_e(t)] \\ y(t) = \mathbf{C}x(t) \end{cases}, \quad (2)$$

where $d_e(t)$ is the equivalent disturbance of $d(t)$ (She 2008).

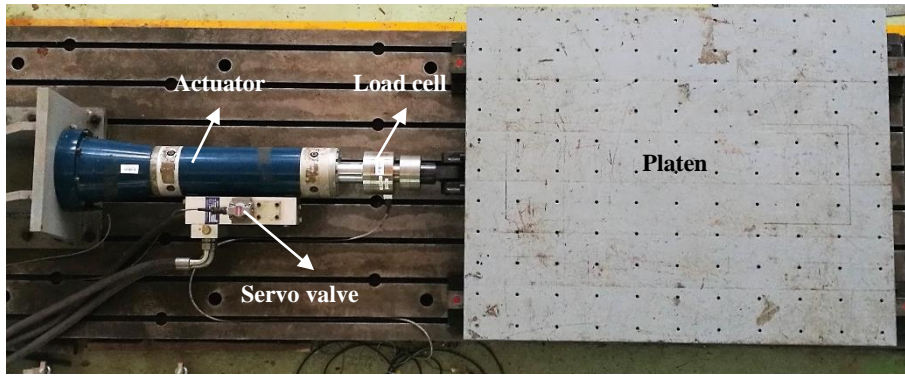


Fig. 2 The hydraulic shaking table at Central South University

2.2 Disturbance compensator

For shaking table composed of actuator, servo valve, and rigid platen, the simplified linear physical model (Guo 2017) is expressed as

$$k_p k_q [u(t) - x_t(t)] = A_p \dot{x}_t(t) + C_{tl} \frac{m \ddot{x}_t(t)}{A_p} + C_{tl} \frac{F_L(t)}{A_p} + \frac{V_t}{4\beta_e} \left[\frac{m \ddot{x}_t(t)}{A_p} + \frac{F_L(t)}{A_p} \right], \quad (3)$$

where $u(t)$ is the input signal of the shaking table, $x_t(t)$, $\dot{x}_t(t)$, $\ddot{x}_t(t)$, $\dddot{x}_t(t)$ are displacement, velocity, acceleration, and jerk of platen respectively, k_q is the flow coefficient of the servo valve, k_p is the proportional gain of inherent actuator control, A_p is the piston area of the actuator, C_{tl} is the leakage coefficient of the actuator, m is the mass of platen, $F_L(t)$ is the interaction force of experimental substructure, V_t is the volume of the actuator, and β_e is the effective bulk modulus.

The experimental substructure is regarded as a disturbance source with platen as payload of the actuator. Choosing the state to be $x_o(t) = [x_t(t) \ \dot{x}_t(t) \ \ddot{x}_t(t)]^T$ and the output to be $y_o(t) = x_t(t)$, the state-space description can be expressed as follows:

$$\begin{cases} \mathbf{A} = \begin{bmatrix} 0 & 1 & 0 \\ 0 & 0 & 1 \\ -\frac{4\beta_e A_p}{mV_t} k_p k_q & -\frac{4\beta_e A_p^2}{mV_t} & -\frac{4\beta_e C_{tl}}{V_t} \end{bmatrix} \\ \mathbf{B} = \begin{bmatrix} 0 \\ 0 \\ \frac{4\beta_e A_p}{mV_t} k_p k_q \end{bmatrix} \quad \mathbf{B}_d = \begin{bmatrix} 0 \\ 0 \\ -\frac{1}{m} \end{bmatrix} \quad d(t) = \begin{bmatrix} 0 \\ 0 \\ \frac{4\beta_e C_{tl}}{mV_t} F_L(t) + \dot{F}_L(t) \end{bmatrix} \end{cases} \quad (4)$$

For the hydraulic shaking table at Central South University, which is shown in Fig. 2, the parameters were identified to be

$$\begin{cases} \mathbf{A} = \begin{bmatrix} 0 & 1 & 0 \\ 0 & 0 & 1 \\ -1.5213e6 & -5.0257e4 & -815.2483 \end{bmatrix} \\ \mathbf{B} = \begin{bmatrix} 0 \\ 0 \\ 1.5213e6 \end{bmatrix} \quad \mathbf{C} = \begin{bmatrix} 1 \\ 0 \\ 0 \end{bmatrix}^T \quad \mathbf{B}_d = \begin{bmatrix} 0 \\ 0 \\ -0.0017 \end{bmatrix} \end{cases}, \quad (5)$$

From Eq. (4), a disturbance is imposed on the same channel with input, which yields the equivalent disturbance estimation $d_e(t)$

$$\begin{cases} d_e(t) = \mathbf{G}_L \mathbf{B}^+ \mathbf{B}_d d(t) \\ \mathbf{B}^+ := \frac{\mathbf{B}^T}{\mathbf{B}^T \mathbf{B}}, \quad \mathbf{G}_L = \frac{1}{Ts+1}, \quad T < 1/(5\omega_r) \end{cases}, \quad (6)$$

where \mathbf{G}_L is a low-pass filter to eliminate the effect of the sensor noise to the estimated equivalent disturbance, ω_r is the highest angular frequency contained in the disturbance $d(t)$.

The interaction force of experimental substructure is calculated by measured platen acceleration $\ddot{x}_t(t)$ and actuator force $F_s(t)$

$$F_L(t) = F_s(t) - m_t \ddot{x}_t(t), \quad (7)$$

Combining Eq.(4), (6), and (7), the control command of the disturbance compensator $u(t)$ is obtained

$$u(t) = u_r(t) - d_e(t), \quad (8)$$

where $u_r(t)$ is the control command of outer-loop control.

2.3 Outer-loop control

The improved shaking table has similar characteristics with the original bare shaking table, which needs to be regulated by an outer-loop controller to achieve high tracking accuracy and short response time. Full-state feedback control in Fig. 3 is adopted as the outer-loop controller. In Eq. (9), the feedback control gain K_f is designed by Ackermann Function (Dorf 2017) for the original shaking table without experimental substructure. The desired poles of Ackermann Function are selected from the left half of the complex plane based on desired transient characteristic of shaking table.

$$\begin{cases} K_f = [1 & 0 & \dots & 0 & 0] P_c^{-1} q(A) \\ P_c = [A^{n-1}B & A^{n-2}B & \dots & AB & B] \end{cases}, \quad (9)$$

where $q(A)$ is the characteristic matrix of target poles.

Steady-state error is compensated by a feedforward gain K_0 which is decided based on the terminal value theorem (Dorf 2017),

$$K_0 = 1 / \left(\frac{b_1 + b_2 + b_3}{1 + a_1^* + a_2^* + a_3^*} \right), \quad (10)$$

where α_i^* ($i = 1, 2, 3$) are characteristic parameters of the target poles, b_j ($j = 1, 2, 3$) are the numerator of the transfer function of Eq. (3).

Then, the control command $u_r(t)$ of the outer-loop controller is obtained by

$$u_r(t) = K_0 x_r(t) - K_f x(t), \quad (11)$$

where state $x(t)$ is observed by Kalman filter.

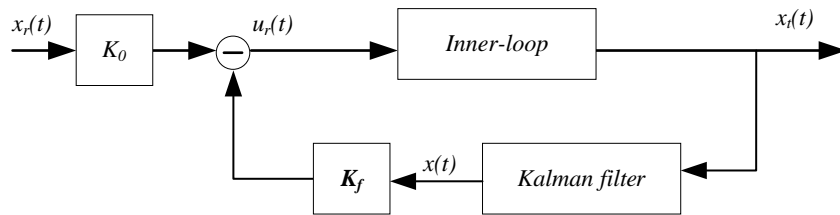


Fig. 3 Framework of disturbance rejection control

3. HYBRID SIMULATION MODEL

The RTHS model describes a China CRH380A train running on a 198.2m long 3-span simply supported bridge at the speed of 350 km/h, as shown in Fig. 4. The bridge is simulated by a finite element model with linear assumptions, and the train is simplified into a quarter vehicle model, in which car-body, bogie, and wheel are represented by masses of 3-degree of freedom.

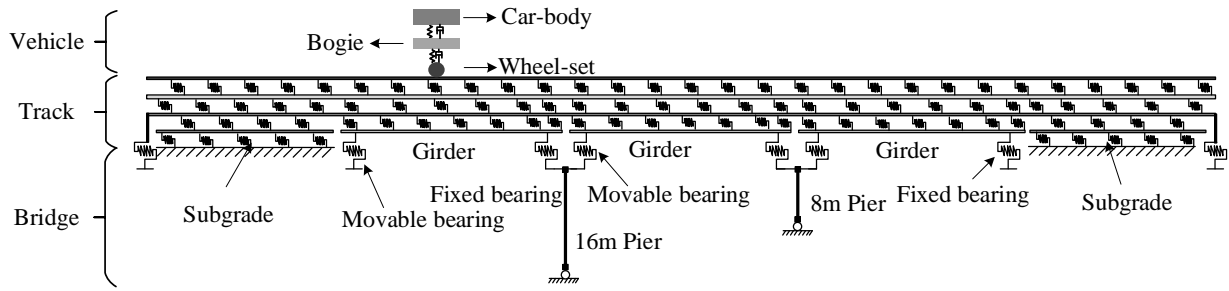


Fig. 4 Model of bridge and train

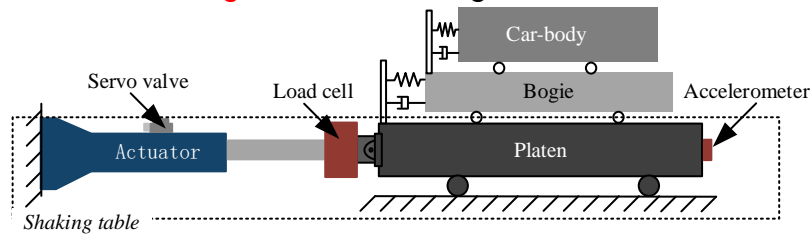


Fig. 5 Uniaxial shaking table fixed with vehicle model

In RTHS, the vehicle is regarded as experimental substructure and the bridge as numerical substructure. Boundary displacement coordination between the two substructures is realized by shaking table, which conveys track deformation of the bridge model to the experimental substructure. As a moving load on the numerical substructure, the interaction force F_I of substructures is obtained by the sum of gravity and inertia force of the vehicle model, as shown in Eq. (12). Assuming the vertical rigid wheel-rail contact relationship, movement of the wheel is consistent with that of shaking table. Then, accelerations of the car-body, bogie, and platen are measured to calculate the inertia force.

$$F_I = (m_c + m_b + m_w)g + m_c\ddot{x}_c + m_b\ddot{x}_b + m_w\ddot{x}_t, \quad (12)$$

where m is the mass, g is the acceleration of gravity, subscribe c, b , and w represent the car-body, the bogie, and the wheel-set separately, k is the stiffness, c is the damping, the designed vehicle parameters are listed in Tab. 1.

Tab. 1 Parameters of vehicle model

Parameter	m_c	m_b	m_w	k_c	k_b	c_c	c_b
Value	4223.25kg	514kg	633.5kg	112500N/m	886000N/m	5000Ns/m	10000Ns/m

Adapted to uniaxial shaking table, the vertical vehicle model is recumbent, as shown in Fig. 5. The shaking table in the RTHS model is identified from the same shaking table at Central South University in Section 2.2. A 3-order nonlinear state-space equation Eq. (13) is adopted as the identification model (Guo 2017), and the identified parameters are listed in Tab. 2.

$$\begin{bmatrix} \dot{x}_1 \\ \dot{x}_2 \\ \dot{x}_3 \end{bmatrix} = \begin{bmatrix} x_2 \\ (x_3 A)/m \\ -\frac{4\beta_e(Ax_2 + C_{tl}x_3)}{V_t} + \frac{4\beta_e C_d \omega k_{sv} k_p (u_1 - x_1)}{V_t \sqrt{\rho}} \sqrt{p_s - \text{sgn}(u - x_1)x_3} \end{bmatrix}, \quad (13)$$

where C_d is the discharge coefficient, ω is the are gradient of spool, k_{sv} is the gain of servo valve, ρ is the density of hydraulic oil, states $x_i (i = 1,2,3)$ represent displacement, velocity, and load pressure of actuator separately.

Tab. 2 Parameters of shaking table model

Parameter	$C_d \omega k_{sv}$	k_p	p_s	ρ	A_p	C_{tl}	V_t	β_e
Value	0.0024	0.25	270Bar	860kg/m ³	3225mm ²	2.87e-10	1.116L	7.8e8Pa

4. SIMULATION RESULTS

On the introduced hybrid simulation model of high-speed railway, the effectiveness of the proposed disturbance rejection control is verified by comparing with that of the outer-loop control only method. Adopted 0.1-5Hz chirp signal as reference signal, tracking displacements of the shaking table fixed with experimental substructure are plotted in Fig. 6. It can be seen that, by rejecting the effect of the experimental substructure, the tracking accuracy of shaking table under the proposed control is better than the one under the outer-loop control only method.

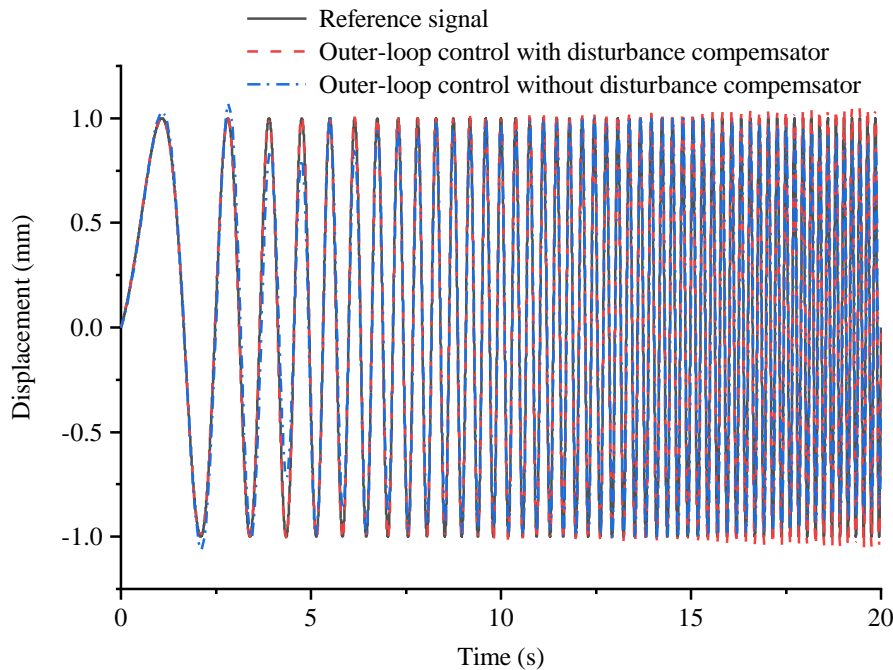


Fig. 6 Tracking displacements of shaking table for 0.1-5Hz chirp signal

A standard RTHS model, in which 1 is set as the transfer function of shaking table, is designated to illustrate the efficiency of shaking table controller. Track deformation of the numerical substructure is sent to shaking table as reference signal. Response displacements of wheel-set in different RTHS models are recorded in Fig. 7. Without the disturbance compensator, the experimental substructure distorted the peak of tracking displacement of the platen, even if the outer-loop control is working. The response displacement of the RTHS model with the disturbance rejection control is closer to that of the standard model.

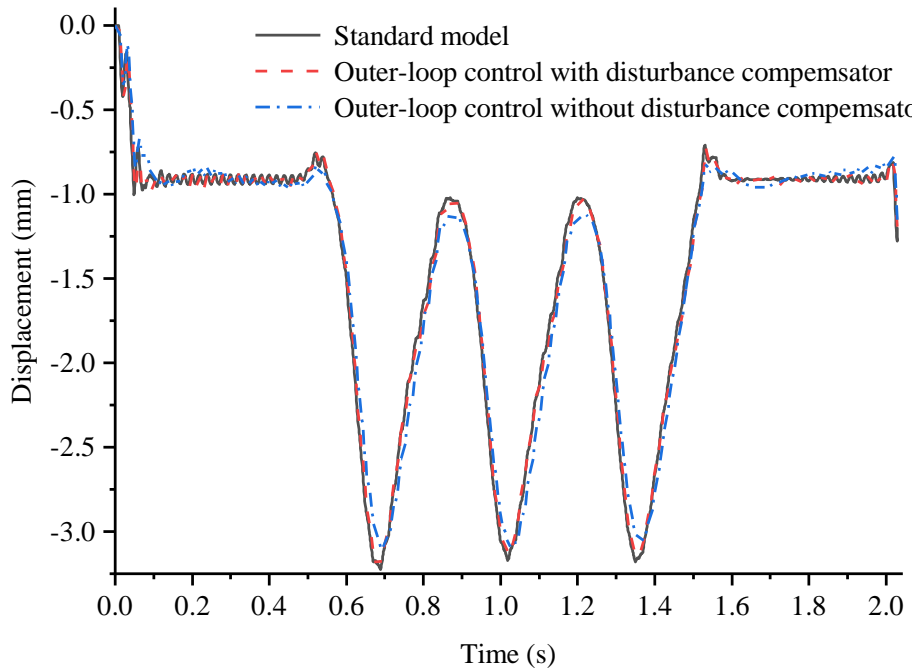


Fig. 7 Response displacement of wheel-set in RTHS

5. CONCLUSIONS

In this paper, a disturbance rejection control composed of a disturbance compensator and an outer-loop control is proposed to compensate for the effect of experimental substructure on displacement tracking of shaking table in real-time hybrid simulation (RTHS). An RTHS model of the high-speed vehicle-bridge coupling vibration is introduced to verify the effectiveness of the proposed control. By comparing the response of shaking table under the proposed control with that under the outer-loop control only method, the following conclusions are drawn: the disturbance compensator limits the tracking displacement distortion of shaking table caused by the experimental substructure; the shaking table under the proposed control showed better tracking accuracy when the 0.1-5Hz chirp signal is used as the reference signal; the dynamic response of RTHS model with the proposed control strategy is closer to that of standard model.

REFERENCES

- Dorf, R.C. and Bishop, R.H. (2017), "Modern Control Systems".
- Dyke, S., Spencer Jr, B., Quast, P., etc. (1995), "Role of control-structure interaction in protective system design," *Journal of Engineering Mechanics*, **121**(2), 322-338.
- Guo, Q. and Jiang, D. (2017). "Nonlinear Control Techniques for Electro-Hydraulic Actuators in Robotics Engineering," CRC Press.
- He, X., Nan, Z., and Guo, W. (2018). "Dynamic Analysis of Train-Bridge Coupling System".
- Iwasaki, M., Ito, K., Kawafuku, M., etc. (2005), "Disturbance observer-based practical control of shaking tables with nonlinear specimen," *IFAC Proceedings Volumes*, **2005**(16), 251-256.
- Qian, Y., Ou, G., Maghareh, etc. (2014), "Parametric identification of a servo-hydraulic actuator for real-time hybrid simulation," *Mechanical Systems & Signal Processing*, **48**(1-2), 260-273.
- Ryu, K.P. and Reinhorn, A.M. (2017), "Real-time control of shake tables for nonlinear hysteretic systems," *Structural Control & Health Monitoring*, **24**(2).
- She, J.H., Fang, M., Ohyama, Y., etc. (2008), "Improving disturbance-rejection performance based on an equivalent-input-disturbance approach," *IEEE Transactions on Industrial Electronics*, **55**(1), 380-389.
- Yang, T., Li, K., Lin, J. Y., Li, Y., etc. (2015) , "Development of high - performance shake tables using the hierarchical control strategy and nonlinear control techniques," *Earthquake Engineering & Structural Dynamics*, **44**(11), 1717-1728.